Cardiovascular Ultrasound

RESEARCH

Open Access

# A new noninvasive evaluation method of pulmonary thromboembolism in rabbits—pulmonary transit time

He Zhang[1], Jianfeng Chen[2], Jiayu Wang[1], Song Kang[1], Yingying Liu[1], Binyang Zhu[1], Xue Mei[1], Xin AI[1], Guangyin Li[1] and Shuangquan Jiang[1*]

## Abstract

**Background and aim** Pulmonary thromboembolism (PTE) is a common cause of cardiovascular death worldwide. Due to its nonspecific clinical symptoms, PTE is easy to be missed or misdiagnosed. Pulmonary transit time (PTT) is a noninvasive cardiopulmonary hemodynamic index, which is the time required for a blood sample to pass through pulmonary circulation. This study is aim to establish a rabbit PTE model using auto-thrombus, evaluating the dynamic changes in a rabbit's heart structure and function at multiple time points before and after modeling by echocardiography and exploring the application value of PTT obtained by contrast enhanced ultrasound (CEUS) in evaluating a PTE model.

**Methods** Twenty-four healthy rabbits were intubated by femoral vein puncture to establish the PTE model. Echocardiography was performed before embolization, 2 h, 24 h, 3 days, 5 days, and 7 days after embolization to obtain conventional ultrasonic parameters. Then, CEUS was performed to obtain the PTT.

**Results** Seventh day after modeling, nineteen rabbits were alive. Compared with pre-modeling, right heart parameters and heart rate in echocardiography were significantly impaired in the acute phase (2 and 24 h after modeling) and gradually returned to normal in the compensatory phase (3, 5, and 7 days after modeling). In contrast with conventional ultrasound parameters, PTT and nPTT revealed a gradually increasing trend at each time point. Receiver operating characteristic (ROC) curve analysis revealed with an extension of molding time, the area under the curve (AUC) of (n)PTT is larger and larger.

**Conclusions** Right heart parameters obtained using conventional echocardiography can accurately indicate changes in the structure and function of the right heart during the acute phase of PTE, while (n)PTT measured by CEUS continues to extend during the acute and compensatory phases of PTE. Therefore, PTT (nPTT) obtained by CEUS is a useful clinical indicator for the diagnosis of PTE and can be utilized as a supplement to conventional echocardiography parameters.

**Keywords** Rabbit, Pulmonary thromboembolism, Disease model, Echocardiography, Contrast enhanced ultrasound, Pulmonary transit time

*Correspondence:
Shuangquan Jiang
23237003@qq.com
Full list of author information is available at the end of the article

**Graphical Abstract**

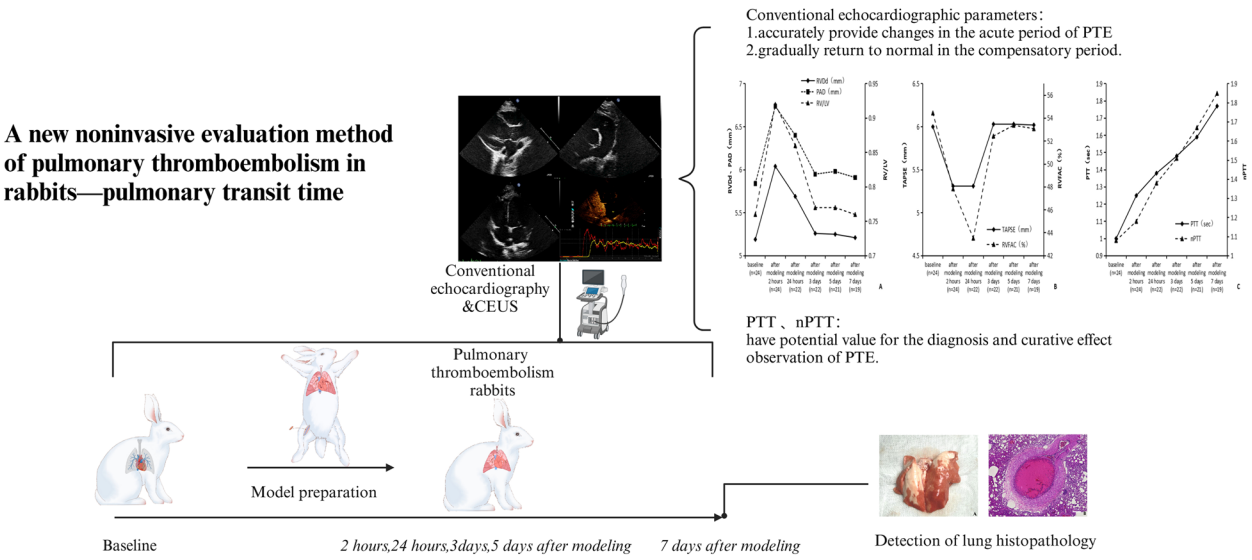


## Introduction

Pulmonary embolism (PE) is a clinical pathophysiological syndrome in which endogenous or exogenous emboli block the pulmonary artery trunk or its branches and cause pulmonary circulation disorder. The clinical symptoms include dyspnea, hemoptysis, syncope, and severe cases may be life-threatening due to right heart failure [1]. Pulmonary thromboembolism (PTE) is the most common type of PE. Its incidence and hospitalization rate are increasing year by year and the thrombus causing PTE mainly originates from the deep veins of lower limbs [2]. PTE is easy to be missed and misdiagnosed because its symptoms are not specific. Computed tomography pulmonary angiography (CTPA) is the gold standard for diagnosing PTE, but it cannot provide detailed information regarding heart structure, function and tissue signature [3]. The application of CTPA is limited for patients with cardiac and renal insufficiency and pregnant and lactating women. Echocardiography is non-invasive and convenient and can dynamically evaluate the hemodynamics of the cardio great vessels and cardiac function in real time [4]. After PTE, emboli lead to narrowing of the main and branch lumen of the pulmonary artery and decreased or blockage of blood flow, which makes pulmonary circulation resistance and pulmonary artery pressure increased. In addition, hypoxia and reflex pulmonary artery contraction can lead to further increases in pulmonary vascular resistance and pulmonary artery pressure. The degree of pulmonary artery pressure increase is closely related to the extent of pulmonary vascular bed obstruction. When the total cross-sectional area of the pulmonary vascular bed blocked by thromboembolus exceeds 30–50%, the pulmonary artery pressure increases significantly. This leads to increased right ventricular afterload, right ventricule dilation and right ventricule dysfunction. Right ventricule enlargement leads to ventricular septum shift to the left side, left heart compressed and cardiac output reduced [5]. PTE can also lead to increased airway resistance, redistribution of pulmonary blood flow, reduced blood flow in the embolized part of the lung, increased blood perfusion in the non-embolized part of the lung, respiratory function changes such as ventilation blood flow imbalance, resulting in pathophysiological changes such as hypoxemia [2, 6]. PTE leads to hemodynamic disorder and respiratory insufficiency, thus, it is rather important to comprehensively evaluate the cardiopulmonary function of PTE patients.

Pulmonary transit time (PTT) is the time required for a blood sample to pass through pulmonary circulation [7]. This is the time for blood to reach the left heart from the right heart [8]. It is a noninvasive index of cardiopulmonary hemodynamics [9]. Research reveals that PTT has a good correlation with cardiac function and pulmonary vascular parameters and can be used as an index to reflect the overall cardiac-pulmonary function [10, 11]. Contrast enhanced ultrasound (CEUS) can visualize the process of contrast agent from the right heart to left heart, thereby yielding PTT. Some researches reveal that PTT evaluated by CEUS has good reliability and

repeatability [11–14]. PTT is helpful for the diagnosis and evaluation of patients with dyspnea and heart failure [9]. It is a noninvasive composite marker of pulmonary hemodynamics and cardiac function in patients with pulmonary hypertension [8]. It is also valuable for prognosis evaluation of patients with myocardial infarction [15]. At present, there are few literature reports on the application of PTT to evaluate PTE. In this study, a rabbit PTE model was established to explore the dynamic changes of ultrasound parameters, particularly PTT, in different periods of PTE and analyze the diagnostic efficiency of each ultrasound parameter.

## Materials and methods

### Experimental animals

Twenty-four healthy Japanese white rabbits, male or female, aged 4–6 months and weighing 3.0 kg–4.5 kg, with an average of 3.7 ± 0.5 kg, were provided by the Experimental Animal Center of the Second Affiliated Hospital of Harbin Medical University (license number: SYXK2019-001). The PTE model was prepared and the changes in ultrasonic parameters at multiple time points were dynamically observed. This experiment was approved by the hospital ethics committee (ethics number: SYDW2021-116).

### Model preparation

#### *Preparation of Autologous Thromboembolism*

Rabbit ears were sterilized with iodophor, and 1 ml of blood was taken from the auricular vein, injected into a sterile dish, and allowed to stand for 30 min. After it solidified, it was placed in a 70℃ water bath box for 15 min. Then, the thrombus was trimmed into five strips with a diameter of 1 mm and a length of 10 mm with ophthalmic scissors and placed in a syringe filled with 5 ml of normal saline for subsequent use.

#### *Establishment of the PTE model*

A small animal anesthesia machine was used (RWD Life Science Co., Ltd, R500IE) and isoflurane was used as an anesthetic; the mask was placed on the nose and mouth of the rabbit, with an oxygen flow of 4L/min and an isoflurane output concentration of 3.5%. The eyelids and cornea of the rabbit were examined to determine whether the anesthesia was successful—when the reflex disappears completely and the limbs become limp the anesthesia is considered successful. Then, the oxygen flow was adjusted to 0.3L/min, and the rabbit continued to be anesthetized. The rabbit was fixed in the supine position on the operating table, shaved in the right inguinal region, disinfected, covered with a hole towel, anesthetized with 1 ml of 2% lidocaine, and separated layer by layer with surgical scissors to fully expose the right femoral vein. After a successful puncture with a 5F trocar, the needle core was pulled out and the cannula was simultaneously pushed into the femoral vein; then the cannula was fixed in the femoral vein with a 4–0 surgical suture. The prepared thrombus strip and the mixed solution of normal saline were pushed into the vein by a bolus injection. The embolus enters the right atrium and ventricle through the inferior vena cava and finally enters the trunk or branch of pulmonary artery to block pulmonary blood flow. Then, the clinical symptoms of rabbits, including breathing amplitude and frequency, color change of nose and mouth, cough, restlessness and convulsion, was observed and recorded. Thereafter, the cannula was pulled out, the femoral vein was ligated at the upper and lower ends to stop bleeding, the incision was sutured, and the model is completed. After modeling, cefoxitin sodium (20 mg/kg) was injected intramuscularly twice a day for seven days to prevent infection.

#### *Evaluation of conventional echocardiography*

The ultrasonic diagnostic instrument uses Philips IE Elite (Philips Healthcare, Bothell, WA, USA) and was equipped with a S12-4 (frequency 4-12MHz) small animal heart probe. Echocardiography was performed at six time points—baseline, 2 h, 24 h, 3 days, 5 days, and 7 days after modeling. After anesthesia, the rabbit was shaved to expose the left chest and connected to a synchronous electrocardiogram. The left lateral position was taken, and left atrial diameter (LAD) and left ventricular end-diastolic diameter (LVDd), left ventricular end-systolic diameter (LVDs), left ventricular ejection fraction (LVEF), and right ventricular end-diastolic diameter (RVDd) were obtained from parasternal long-axis view. The pulmonary artery diameter (PAD) was obtained from parasternal short-axis view of the aorta. The right atrial diameter (RAD) and the right/left ventricular end-diastolic diameter ratio (RV/LV), right ventricular fractional area change (RVFAC), and tricuspid annular plane systolic excursion (TAPSE) were obtained from the apical four-chamber view. Each index was measured three times and averaged.

#### *Contrast enhanced ultrasound evaluation*

The ultrasound contrast agent (UCA) used was SonoVue (Bracco, Milan, Italy). 5 ml of 0.9% normal saline was injected into the dry powder bottle of SonoVue and evenly mixed. UCA was injected into the right auricular vein through the reserved indwelling needle at a dose of 0.1 ml/kg [16] and then washed with 0.5 ml normal saline. Thereafter, the ultrasonic parameters were adjusted: the dynamic range was 50 dB–55 dB, mechanical index was 0.3–0.5, and gain was 70%–75% to obtain the best CEUS image. The complete dynamic video of the UCA appearing

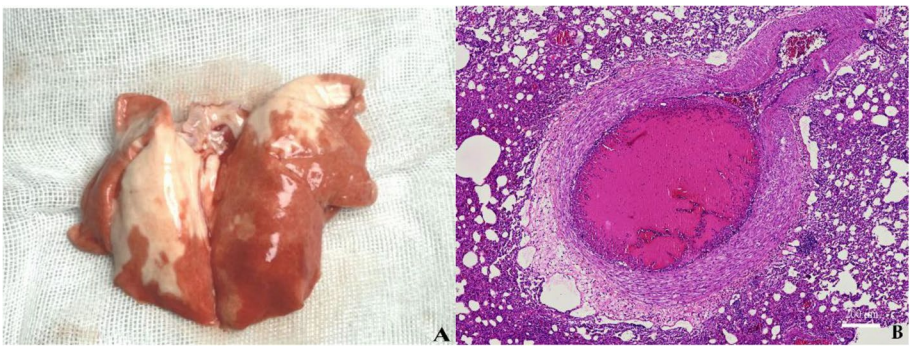


**Fig. 1** HE staining of gross lung specimen and pathological tissue in a rabbit model of pulmonary thromboembolism (×50). (A) The gross specimen of the lung revealed that the lung was slightly enlarged and red and white, and the area of the right pulmonary embolism was larger than that of the left lung; (B) HE staining in the embolic area revealed a pink cylindrical thrombus embolus in the lumen, and the alveolar wall and septum around the embolic site were thickened

in the right heart and the left heart in sequence was stored in the apical four-chamber view. QLab software was used for post-processing analysis, and the region of interest (ROI) was drawn in the middle of left atrium and right atrium respectively, with a size of 1.00 $mm^2$–1.16 $mm^2$, and the time intensity curve (TIC) of the right atrium and left atrium was automatically generated. The time interval between the first appearance of the UCA in the right atrium and the left atrium—that is, PTT—was obtained by combining the turning point of TIC sudden rise with the "frame counting" technology [10]. In addition, in order to reduce the influence of heart rate (HR) on PTT, normalized PTT (nPTT) was calculated. The nPTT is calculated by multiplying PTT by the number of heartbeats per second (nPTT = PTT × HR/60) [12].

#### *Detection of lung histopathology*

Samples were taken immediately after ultrasonic image acquisition was completed seven days after modeling. Normal saline was continuously perfused through the right ventricle and pulmonary artery until the lung tissue turned white; then, the heart and lung tissue were extracted and the pulmonary tissue morphology, color changes, and the location of embolization was observed. Samples were taken from the PTE area and fixed in paraformaldehyde for 24 h. After paraffin embedding, sectioning, and hematoxylin–eosin (HE) staining, the morphology of the embolus in the pulmonary artery and the histological changes of the surrounding alveolar cells were observed. All rabbits were euthanized after the completion of the study.

### Statistical analysis

Statistical analysis was performed by using IBM SPSS 26.0 software. The Shapiro–Wilk test was used to test the normality of the data distribution. The continuous data are represented by mean and standard deviation (normal distribution). Repeated measures analysis of variance was used to compare continuous variables at each time point, and Bonferroni method was used to compare them in pairs. $P < 0.05$ indicates that the difference is statistically significant. The ROC curve was used to analyze the sensitivity and specificity and the area under curve (AUC) of the parameters of the right heart, PTT and nPTT.

## Results

### Preparation of a rabbit PTE model

All 24 rabbits survived 2 h after the preparation of PTE model; 2 died of anesthesia accident at 1 day and another 2 died at 7 days after modeling for the same reason, 1 died of excessive injection of UCA at 5 days after modeling, and 19 rabbits survived at 7 days after modeling. Immediately after the preparation of the PTE model, all rabbits displayed restlessness, increased breathing extent and frequency, and nasal alar agitation. Among these, 13 rabbits presented with cyanosis in the mouth and nose, 7 rabbits presented with convulsions, and 6 rabbits presented with severe cough. The above symptoms were gradually relieved 20–30 min after the preparation of the PTE model.

### Pathological results of lung tissue

The lung of PTE rabbits was swollen and red and white. The normal lung tissue after lavage with normal saline was milky white, and the lung tissue at the embolism site was dark red. The crimson region was mostly located in the middle and lower portions of both lungs. In a few lung specimens, the crimson regions covered both lungs, and most emboli are embolized in the right lung lobus diaphragmaticus. Microscopically, pink thrombus embolus was seen in the lumen of blood vessel. The arterial

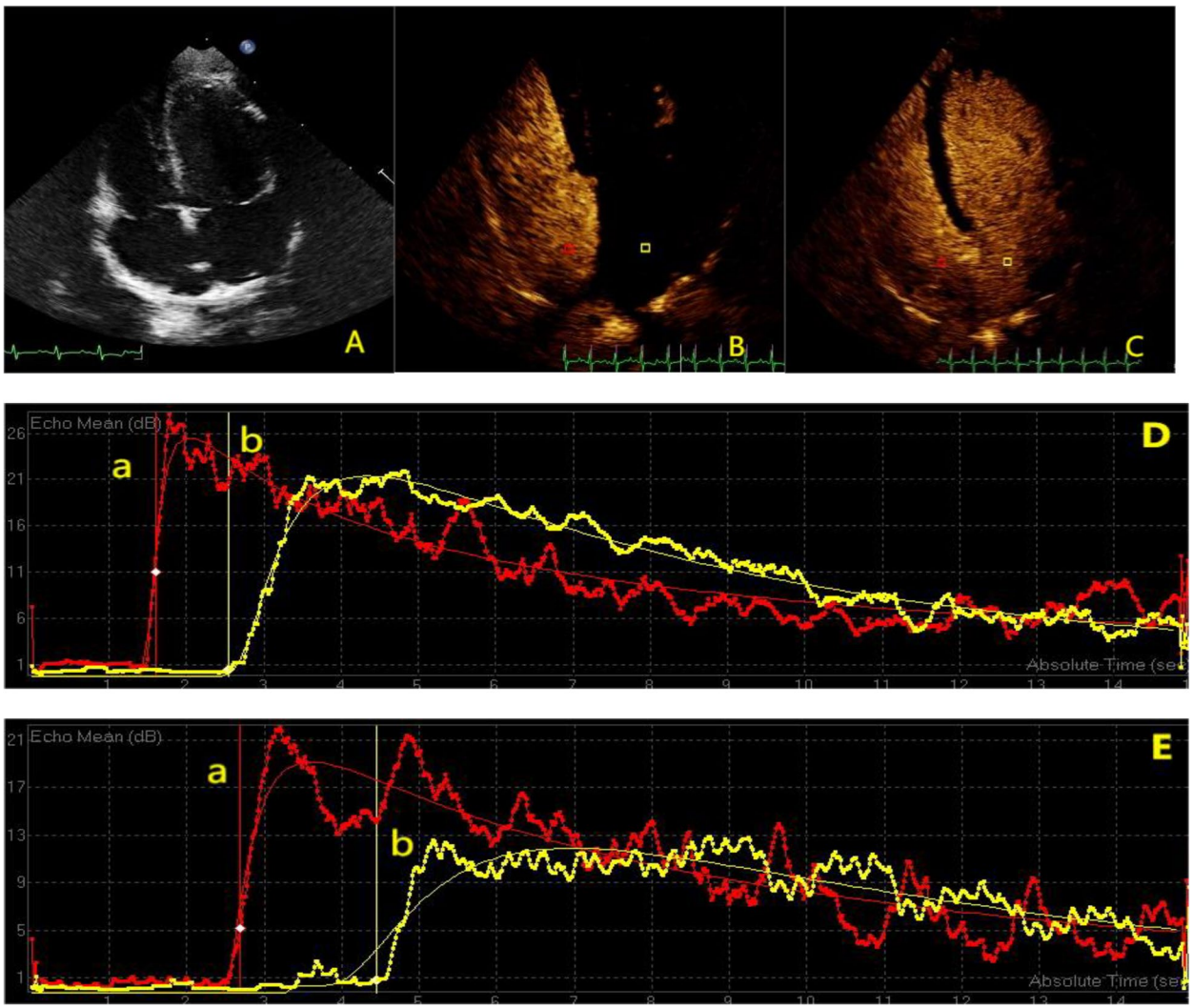


**Fig. 2** Two-dimensional and contrast enhanced ultrasound (CEUS) images of rabbit apical four-chamber view. (A)Apical Four-chamber view of the normal rabbit; (B) CEUS image, in which the UCA was filled in the right heart; (C) CEUS image, in which the UCA was then filled in the left heart. The red and yellow rectangular frames are the regions of interest in the right atrium and the left atrium, respectively, and the TIC was generated; (D) The time point corresponding to line A represents the time when the UCA first appeared in the right atrium, and the time point corresponding to line B represents the time when the UCA first appeared in the left atrium, and the time interval between them is PTT. This picture is TIC of a normal rabbit and PTT of normal rabbits were 0.867s. (E) This picture is TIC of a rabbit at seventh day after PTE and PTT were significantly prolonged to 1.768s

wall at the embolic site was thickened, and inflammatory cells were infiltrated inside. The alveolar wall and alveolar septum around it were thickened, and the alveoli collapse and inflammatory cells were infiltrated inside the alveolar septum (Fig. 1).

### Dynamic changes of echocardiographic parameters before and after modeling

All rabbits clearly displayed the standard views of the heart (Fig. 2).

Compared with baseline, the differences in RVDd, PAD, RVFAC, RV/LV, TAPSE, HR, PTT, and nPTT after PTE model preparation were statistically significant ($P<0.01$). There was no significant difference in LAD, LVDd, LVDs, LVEF, and right atrial diameter ($P>0.05$) (Table 1).

The parameters with statistical significance for the above differences are further compared at each time point after PTE model preparation with baseline, and the results are presented in Table 2. RVDd, PAD and RV/LV increased to the peak at two hours after modeling and then decreased gradually, and the differences between 2

**Table 1** Comparison of echocardiographic parameters at different time points in a rabbit model of pulmonary thromboembolism

| Parameter | Time point of ultrasound examination (mean standard deviation) | | | | | | F | *P* value |
|---|---|---|---|---|---|---|---|---|
| | Baseline (*n* = 24) | After modeling 2 h (*n* = 24) | After modeling 24 h (*n* = 22) | After modeling 3 days (*n* = 22) | After modeling 5 days (*n* = 21) | After modeling 7 days (*n* = 19) | | |
| LAD(mm) | 9.48 ± 1.40 | 10.08 ± 0.80 | 9.88 ± 0.75 | 10.05 ± 0.82 | 9.97 ± 1.09 | 10.09 ± 1.26 | 2.467 | 0.77 |
| LVDd(mm) | 15.63 ± 1.39 | 15.56 ± 1.67 | 15.33 ± 1.53 | 15.27 ± 1.40 | 15.08 ± 1.62 | 15.36 ± 1.37 | 3.113 | 0.095 |
| LVDs(mm) | 10.05 ± 1.06 | 9.97 ± 0.96 | 9.61 ± 1.21 | 9.56 ± 0.97 | 9.81 ± 0.83 | 9.92 ± 0.99 | 2.196 | 0.104 |
| LVEF(%) | 71.06 ± 1.65 | 70.10 ± 2.81 | 70.09 ± 2.74 | 68.74 ± 1.84 | 69.91 ± 1.71 | 69.96 ± 2.15 | 2.637 | 0.05 |
| RAD-LR(mm) | 9.91 ± 2.58 | 10.98 ± 1.30 | 10.07 ± 1.54 | 10.19 ± 1.33 | 10.14 ± 1.55 | 9.96 ± 1.26 | 1.646 | 0.204 |
| RAD-UD(mm) | 10.53 ± 1.15 | 10.96 ± 0.90 | 10.45 ± 0.93 | 10.34 ± 0.95 | 10.30 ± 1.28 | 10.39 ± 1.27 | 2.44 | 0.072 |
| RVDd(mm) | 5.19 ± 0.19 | 6.04 ± 0.28 | 5.69 ± 0.28 | 5.26 ± 0.16 | 5.25 ± 0.14 | 5.21 ± 0.20 | 119.10 | 0.000** |
| PAD(mm) | 5.84 ± 0.33 | 6.74 ± 0.23 | 6.40 ± 0.65 | 5.95 ± 0.28 | 5.98 ± 0.24 | 5.91 ± 0.30 | 21.973 | 0.000** |
| RVFAC(%) | 54.45 ± 4.39 | 47.84 ± 2.72 | 43.53 ± 4.03 | 52.44 ± 5.38 | 53.38 ± 4.91 | 53.08 ± 4.78 | 30.113 | 0.000** |
| RV/LV | 0.76 ± 0.04 | 0.92 ± 0.74 | 0.86 ± 0.06 | 0.77 ± 0.07 | 0.77 ± 0.05 | 0.76 ± 0.05 | 41.444 | 0.000** |
| TAPSE(mm) | 6.00 ± 0.25 | 5.31 ± 0.74 | 5.31 ± 0.52 | 6.03 ± 0.04 | 6.02 ± 0.04 | 6.03 ± 0.03 | 19.274 | 0.000** |
| HR(bpm) | 269 ± 11 | 237 ± 31 | 251 ± 21 | 256 ± 14 | 262 ± 12 | 261 ± 16 | 11.012 | 0.000** |
| PTT(sec) | 1.00 ± 0.09 | 1.25 ± 0.21 | 1.38 ± 0.15 | 1.48 ± 0.15 | 1.59 ± 0.18 | 1.77 ± 0.19 | 115.19 | 0.000** |
| nPTT | 3.65 ± 0.77 | 4.48 ± 0.80 | 5.70 ± 0.73 | 6.30 ± 0.66 | 6.94 ± 0.86 | 7.69 ± 1.01 | 95.543 | 0.000** |

*LAD* left atrial diameter, *LVDd* left ventricular end-diastolic diameter, *LVDs* left ventricular end-systolic diameter, *RAD-LR* left and right diameter of right atrium, *RAD-UD* up and down diameter of right atrium, *RVDd* right ventricular end-diastolic diameter, *PAD* pulmonary artery diameter, *RVFAC* right ventricular area change fraction, *RV/LV* right/left ventricular end-diastolic diameter ratio, *TAPSE* tricuspid annular plane systolic excursion, *HR* heart rate, *PTT* pulmonary transit time, *nPTT* normalized pulmonary transit time

* $P < 0.05$

** $P < 0.01$

h after modeling and baseline as well as 24 h after modeling and baseline were statistically significant ($P < 0.05$). RVFAC, TAPSE, and HR decreased after modeling, reached the lowest at 24 h, and then gradually increased; and the differences between 2 h after modeling and baseline as well as 24 h after modeling and baseline were statistically significant ($P < 0.05$). There was no significant difference in the above parameters between 3 days, 5 days, and 7 days after PTE and baseline ($P > 0.05$) (Fig. 3A and B). In contrast to conventional ultrasound parameters, PTT and nPTT revealed a continuous upward trend at each time point after operation, and the differences were statistically significant compared with those before modeling ($P < 0.05$) (Fig. 3C).

### ROC curve analysis of echocardiographic parameters

In order to evaluate the diagnostic efficiency of right ventricular parameters, PTT and nPTT for PTE, the ROC curves of the above parameters were analyzed (RVDd, PAD, RVFAC, RV/LV, TAPSE, PTT, and nPTT) at various time points after PTE. At 2 h and 24 h after modeling, the AUC of all parameters was greater than 0.70, and the AUC of PAD was the largest at 2 h after modeling, which was 0.879. The AUC of nPTT was the highest at 24 h after modeling, which was 0.898, with sensitivity and specificity of 0.818 and 0.875, respectively. On the third, fifth, and seventh day after modeling, the AUCs of PTT and nPTT were larger than 0.85, and the sensitivity and specificity were higher. With the extension of time after PTE, the AUC of PTT and nPTT gradually increased (Table 3 and Fig. 4).

## Discussion

Venous thromboembolism is one of the three acute cardiovascular syndromes in the world, and its incidence is second only to myocardial infarction and stroke; it is often manifested as deep venous thrombosis and/or PE in clinic [17]. Epidemiological studies reveal that the annual incidence rates of PE are 39–115/100,000, and the incidence rates of deep venous thrombosis are 53–162/100,000 [18, 19]. The incidence of PE worldwide is increasing year by year [20–25], according to statistics, in the last decades, the incidence rate of PE in England increased from 50.2 to 97.8 per 100,000 population; in America the rate increased from 38.3 to 65.8 per 100,000 population. At the same time, PE has a high mortality rate, which ranks among the leading causes of death from cardiovascular diseases [19]. Timely diagnosis and treatment are very important to improve the prognosis and survival rate of PE patients.

Rabbits are gentle, their heart and lung structures are similar to those of humans, and their fibrinolysis system

**Table 2** Paired comparison of echocardiographic indexes at different time points in a rabbit model of pulmonary thromboembolism and baseline

| | Baseline | After modeling 2 h | | After modeling 24 h | | After modeling 3 days | | After modeling 5 days | | After modeling 7 days | |
|---|---|---|---|---|---|---|---|---|---|---|---|
| **Parameter** | **Average value** | **Average value** | ***P* value** | **Average value** | ***P* value** | **Average value** | ***P* value** | **Average value** | ***P* value** | **Average value** | ***P* value** |
| RVDd(mm) | 5.19 | 6.04 | 0.000** | 5.69 | 0.000** | 5.26 | 0.95 | 5.25 | 1.0 | 5.21 | 1.0 |
| PAD(mm) | 5.84 | 6.74 | 0.000** | 6.40 | 0.017* | 5.95 | 0.661 | 5.98 | 0.524 | 5.91 | 0.583 |
| RVFAC(%) | 54.45 | 47.84 | 0.000** | 43.53 | 0.000** | 52.44 | 0.692 | 53.38 | 1.0 | 53.08 | 0.482 |
| RV/LV | 0.76 | 0.92 | 0.000** | 0.86 | 0.004** | 0.77 | 0.826 | 0.77 | 0.943 | 0.76 | 0.773 |
| TAPSE(mm) | 6.00 | 5.31 | 0.012* | 5.31 | 0.001** | 6.03 | 0.057 | 6.03 | 0.075 | 6.02 | 0.059 |
| HR(bpm) | 269 | 237 | 0.000** | 251 | 0.022* | 256 | 0.126 | 262 | 0.502 | 261 | 0.619 |
| PTT(sec) | 1.00 | 1.25 | 0.001** | 1.38 | 0.000** | 1.48 | 0.000** | 1.59 | 0.000** | 1.77 | 0.000** |
| nPTT | 3.65 | 4.48 | 0.032* | 5.70 | 0.000** | 6.30 | 0.000** | 6.94 | 0.000** | 7.69 | 0.000** |

* $P < 0.05$

** $P < 0.01$ compared with baseline

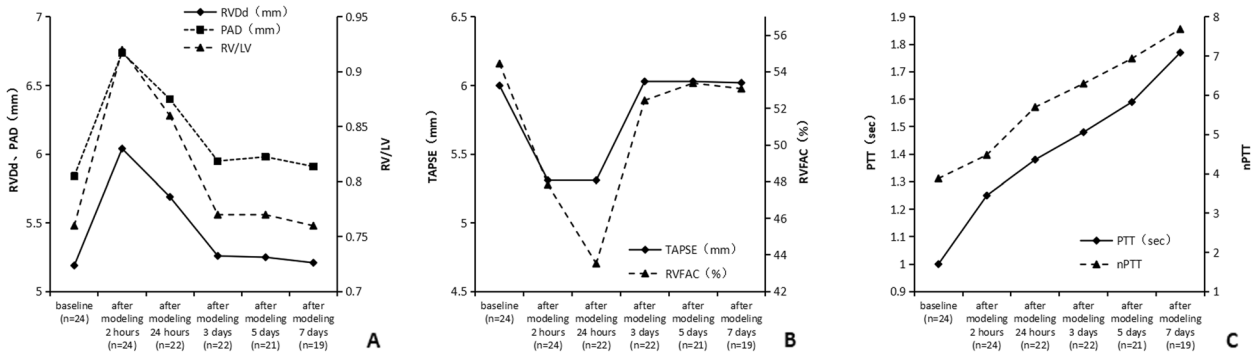


**Fig. 3** Variation trend of ultrasonic parameters at each time point after the preparation in a rabbit model of pulmonary thromboembolism

is also close to that of humans [26]. Therefore, rabbits were selected as experimental animals in this study. Previous studies [27] have revealed that the rabbit PTE model can accurately simulate the process of human PTE and provide a basis for clinical research of human PTE. Currently, blood clots, microparticles, gelatin sponges, and suture segments can be used as emboli to establish PE models [28]. Injection routes include femoral vein, external jugular vein, and auricular vein. In this study, autologous thrombus was selected as the embolus, and the thrombus embolus was injected through the femoral vein. The embolus returned to the right heart with the blood flow of the inferior vena cava and finally entered the pulmonary artery. The advantage of this is that it can simulate the pathophysiological process of deep vein thrombosis in human lower limbs shedding to the right heart. Two hours after modeling, the survival rate of rabbits was 100%. Thrombo-emboli were found in lung gross specimens, most of which were embolized lobus diaphragmaticus of both lungs, and the right lung was more embolized than the left lung. HE staining revealed dense thrombo-emboli and infiltration of inflammatory cells in the lumen of pulmonary artery branches, which was confirmed by anatomy and histopathology.

It is suggested that echocardiography should be performed within 24 h after PTE diagnosis [29]. Patients treated with thrombolysis within 48 h of PTE had the greatest benefit [30]. Clinically, the 48-h is the boundary, which is divided into acute period and compensatory period. In this study, referring to the above criteria, 2 h and 24 h after modeling of PTE were set as the acute phase, while 3 days, 5 days and 7 days after modeling were set as the compensatory phase of PTE. Routine echocardiography and CEUS examination were performed at various time points in the acute and compensatory phases to observe the dynamic changes in cardiac

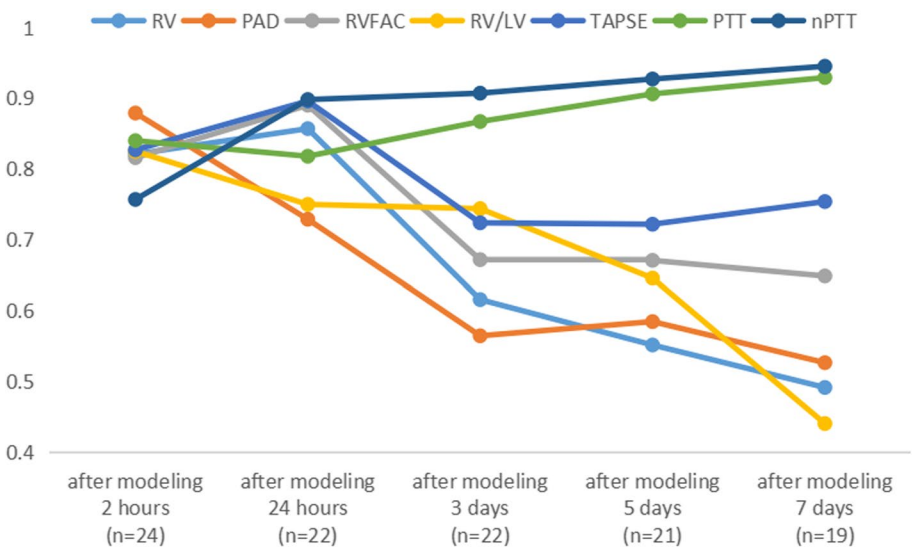


**Fig. 4** The AUC variation trends of right heart parameters and (n)PTT at each time point in a rabbit model of pulmonary thromboembolism

**Table 3** The diagnostic efficiency of right heart parameters and (n)PTT in a rabbit model of pulmonary thromboembolism at each time point

| Parameter | After modeling 2 h | After modeling 24 h | After modeling 3 days | After modeling 5 days | After modeling 7 days |
|---|---|---|---|---|---|
| | Area under curve (sensitivity/specificity) | | | | |
| RVDd(mm) | 0.821 (0.792/0.917) | 0.857 (0.955/0.833) | 0.616 (0.591/0.708) | 0.552 (0.286/0.792) | 0.492 (0.842/0.25) |
| PAD(mm) | 0.879 (0.792/0.857) | 0.729 (0.500/0.958) | 0.565 (0.773/0.375) | 0.585 (0.810/0.458) | 0.527 (0.789/0.333) |
| RVFAC(%) | 0.816 (0.625/0.958) | 0.890 (0.773/0.875) | 0.672 (0.409/0.958) | 0.671 (0.476/0.958) | 0.649 (0.684/0.667) |
| RV/LV | 0.825 (0.75/0.958) | 0.750 (0.591/0.958) | 0.744 (0.682/0.833) | 0.646 (0.619/0.708) | 0.441 (0.263/0.833) |
| TAPSE(mm) | 0.827 (0.833/0.75) | 0.896 (0.727/0.958) | 0.724 (0.682/0.75) | 0.722 (0.714/0.75) | 0.754 (0.737/0.75) |
| PTT(sec) | 0.840 (0.875/0.75) | 0.818 (0.864/0.708) | 0.867 (0.818/0.875) | 0.906 (0.81/0.917) | 0.929 (0.947/0.875) |
| nPTT | 0.757 (0.583/0.875) | 0.898 (0.818/0.875) | 0.907 (0.818/0.958) | 0.927 (0.952/0.875) | 0.945 (0.947/0.958) |

structure and function, particularly PTT. Thus far, there is no such report.

In the acute period of PTE, pulmonary vascular resistance increased under the combined action of pulmonary artery obstruction and hypoxic vasoconstriction [31], which in turn leads to an increase of right ventricular afterload and right ventricular dilatation, and a decrease in the right ventricular systolic function. The results of this study reveal that in the acute phase of PTE, compared with before modeling, PAD, RVDd, RV/LV are increased to different extents, while RVFAC and TAPSE are decreased. These results indicate that in the acute period of PTE, echocardiography can accurately reflect the changes in cardiac structure and function and provide auxiliary information for clinic practice. During the compensatory period of PTE, the right ventricular myocardial contractility increased through the Frank-Starling mechanism. Simultaneously, the activation of the nerve-humoral system produces positive chronotropic and inotropic effects and maintains the output of the right heart. These compensation mechanisms and vasoactive substances constitute systemic vasoconstriction, and the systemic blood pressure returns to normal and stable [18, 32]. However, echocardiography has low sensitivity to PTE with stable hemodynamics [18]. The results of this study revealed that at three, five, and seven days after molding, the indexes such as PAD, RVDd, RV/LV, HR, RVFAC, and TAPSE measured by conventional ultrasound have no statistical significance compared with those before modeling. This indicates that in the compensatory period of PTE, conventional echocardiography cannot make an accurate diagnosis of the disease, which is consistent with previous research results [29].

Different from conventional ultrasound parameters, PTT is a parameter of pulmonary circulation, which refers to the time for a certain amount of blood to pass through pulmonary circulation and its prolongation is related to the dysfunction of both ventricles and the increase of pulmonary vascular resistance [33]. Prior studies [28, 34, 35] using PTT to evaluate heart failure, hepatopulmonary syndrome, pulmonary hypertension, and other diseases. However, there is little research data on PTE. The results of this study revealed that PTT and nPTT increased gradually with the extension of the model preparation time, which may be due to the continuous increase in pulmonary vascular resistance and pressure caused by PTE, and pulmonary blood flow was mainly determined by cardiac function and pulmonary hemodynamics [36, 37]. The change in hemodynamics affects the pulmonary transport of the ultrasound contrast agent [8]. Although the precise physiological basis of the relationship between PTT and pulmonary hemodynamics in acute PTE is not clear, the comprehensive factors such as the increase in pulmonary wedge pressure, the expansion of the pulmonary vascular bed, the increase in blood perfusion in the non-occluded part of the pulmonary vessels, and the decrease in cardiac output caused by left ventricular compression may lead to the prolongation of PTT. Previous literature [38] reveals that PTT in PTE patients is obviously prolonged, which is consistent with the results of this study. PTT and nPTT can accurately identify PTE in both the acute and compensatory periods.

PTT can be measured by various imaging methods. The traditional pulmonary thermodilution involves obtaining the arterial thermodilution curve and PTT after injecting cold physiological saline into the central vein. However, this method needs the insertion of thermodilution catheter and the installation of the temperature sensor, which is laborious and time-consuming [14]. The first-pass perfusion images are obtained by CT and PTT is calculated by subtracting the peak time of the left ventricular curve from the peak time of the right ventricular curve, which can identify patients with decreased ejection fraction and pulmonary hypertension. However, CT has limitations such as low time resolution and radiation exposure [34]. Dynamic contrast enhanced magnetic resonance imaging (MRI) can be utilized to detect the difference between patients with heart failure and healthy subjects through PTT determined by the time interval when the contrast agent first arrives in the right and left ventricles [39]. However, MRI technology is expensive and requires the patient to hold their breath, so it cannot be utilized for animals and patients who cannot breathe spontaneously. Through pulmonary angiography, PTT determined by observing the turbidity peak time between the contrast agent entering the pulmonary trunk and the left atrium can be used to diagnose hepatopulmonary syndrome [35]. However, it is invasive, expensive, and taboo for pregnant women and people with renal insufficiency. CEUS is real-time, convenient, and can be operated at bedside. Previous studies [40–42] reveal that the measurement of PTT by CEUS has good feasibility and reproducibility, it is consistent with the PTT obtained by MRI, and does not depend on the size and position of ROI; thus, CEUS is selected to obtain PTT in this study. Currently, SonoVue is widely used in clinical practice, and the incidence of side effects is extremely low [43]. It is also well tolerated in patients with severe heart failure and pulmonary hypertension [44].

The analysis of the ROC curve reveals that the AUC of PAD is the largest at two hours after the model is created, and the AUC of three conventional echocardiographic parameters—RVDd, RVFAC, and TAPSE—are all above 0.85 at 24 h after the model is created. Moreover, it is evident that in the acute period of PTE, although it is difficult to directly display the embolus in the pulmonary artery trunk and branches, the conventional ultrasound parameters sensitively reflect the changes in hemodynamics, and nPTT also shows good diagnostic efficiency at 24 h after the model is made. On the third, fifth, and seventh days after PTE modeling, the AUC of PTT and nPTT were larger than other parameters, and both were above 0.85, with high sensitivity and specificity; morever, the AUC increased with time. PTT obtained by CEUS is expected to supplement conventional ultrasound examination and make up for its low sensitivity in detecting pulmonary embolism [4, 45].

This study has the following limitations. First, the small sample size may affect the accuracy of the research results. Second, this study only confirmed the successful establishment of the pulmonary embolism model through gross anatomy and pathological examination; no other imaging examinations were conducted to evaluate the relationship between embolic area and PTT. Third, the hemodynamic parameters of rabbits, such as pulmonary artery pressure and pulmonary vascular resistance, were not invasively evaluated in this study. Fourth, this study did not evaluate the relationship between the prolongation of PTT and the prognosis of pulmonary embolism. Fifth, we did not research whether there were sex differences in PTT about rabbits. Sixth, lack of echocardiographic assessment of pulmonary hypertension using tricuspid regurgitation velocity.

## Conclusion

The rabbit PTE model can be successfully established by utilizing an autologous thrombus. Conventional echocardiographic parameters can accurately provide changes in the structure and function of the right heart in the acute period of PTE, which is of great significance for the diagnosis of PTE; however, the ultrasonic parameters gradually return to normal in the compensatory period. PTT (nPTT) measured by CEUS is continuously prolonged in the acute and compensatory periods of PTE, which has potential value for the diagnosis and curative effect observation of PTE.

#### Acknowledgements

The authors thank the editor from Scribendi Co. for providing language help and writing assistance.

#### Financial disclosures

The work was supported by the Natural Science Foundation of Heilongjiang Province [Grant number LH2022H026 and number LH2022H025].

#### Authors' contributions

He Zhang was a major contributor in writing the manuscript. Jianfeng Chen prepared a rabbit model of pulmonary thromboembolism. Jiayu Wang and Song Kang acquired the ultrasonic image of rabbits. Yingying Liu, Binyang Zhu, Xue Mei, Xin Ai and Guangyin Li participated in the data collection and analysis of the article. Shuangquan Jiang participated in the experimental design and guidance. All authors read and approved the final manuscript.

#### Data availability

No datasets were generated or analysed during the current study.

## Declarations

#### Ethics approval and consent to participate

The study was approved by the Second Affiliated Hospital of Harbin Medical University Ethics Committee (ethics number: SYDW2021-116).

**Competing of interests**
The authors declare no competing interests.

**Author details**
[1]Department of Ultrasound Medicine, The Second Affiliated Hospital of Harbin Medical University, 146 Baojian Road, Harbin, Heilongjiang Province 150086, China. [2]Laboratory Animal Center, The Second Affiliated Hospital of Harbin Medical University, Harbin, Heilongjiang Province 150086, China.

Received: 26 August 2024 Accepted: 26 February 2025
Published online: 12 March 2025

**References**

1. Carson JL, Kelley MA, Duff A, et al. The clinical course of pulmonary embolism. N Engl J Med. 1992;326(19):1240–5.
2. Pulmonary embolism and pulmonary vascular Disease Group of Chinese Medical Association Respirtory Branch, pulmonary Vascular Disease Working Committee of Chinese Medical Doctor Association Respirtory Physician Branch, National Pulmonary embolish and pulmonary vascular disease Prevention and Treatment Collaboratoin Group. The clinical practice guideline for diagnosis,treatment and prevention of pulmonary thromboembolism. Nat Med J China. 2018;98(14):1060–87.
3. Gong C, Guo X, Wan K, et al. Corrected MRI Pulmonary Transit Time for Identification of Combined Precapillary and Postcapillary Pulmonary Hypertension in Patients With Left Heart Disease. J Magn Reson Imaging. 2023;57(5):1518–28.
4. Platz E, Hassanein AH, Shah A, et al. Regional right ventricular strain pattern in patients with acute pulmonary embolism. Echocardiography. 2012;29(4):464–70.
5. Marcus JT, Gan CT, Zwanenburg JJ, et al. Interventricular mechanical asynchrony in pulmonary arterial hypertension: left-to-right delay in peak shortening is related to right ventricular overload and left ventricular underfilling. J Am Coll Cardiol. 2008;51(7):750–7.
6. Burrowes KS, Clark AR, Tawhai MH. Blood flow redistribution and ventilation-perfusion mismatch during embolic pulmonary arterial occlusion. Pulm Circ. 2011;1(3):365–76.
7. Streitberger A, Hocke V, Modler P. Measurement of pulmonary transit time in healthy cats by use of ultrasound contrast media "Sonovue®": feasibility, reproducibility, and values in 42 cats. J Vet Cardiol. 2013;15(3):181–7.
8. Skrok J, Shehata ML, Mathai S, et al. Pulmonary arterial hypertension: MR imaging-derived first-pass bolus kinetic parameters are biomarkers for pulmonary hemodynamics, cardiac function, and ventricular remodeling. Radiology. 2012;263(3):678–87.
9. Segeroth M, Winkel DJ, Strebel I, et al. Pulmonary transit time of cardiovascular magnetic resonance perfusion scans for quantification of cardiopulmonary haemodynamics. Eur Heart J Cardiovasc Imaging. 2023;24(8):1062–71.
10. Brittain EL, Doss LN, Saliba L, et al. Feasibility and Diagnostic Potential of Pulmonary Transit Time Measurement by Contrast Echocardiography: A Pilot Study. Echocardiography. 2015;32(10):1564–71.
11. Herold IH, Saporito S, Bouwman RA, et al. Reliability, repeatability, and reproducibility of pulmonary transit time assessment by contrast enhanced echocardiography. Cardiovasc Ultrasound. 2016;14:1.
12. de Lepper AGW, Herold IHF, Saporito S, et al. Noninvasive pulmonary transit time: A new parameter for general cardiac performance. Echocardiography. 2017;34(8):1138–45.
13. Wang HM, Zheng XZ, Sun F. Differential diagnosis of acute pulmonary embolism using contrast echocardiography. Med Ultrason. 2022;24(3):323–8.
14. Herold IH, Soliman Hamad MA, van Assen HC, et al. Pulmonary blood volume measured by contrast enhanced ultrasound: a comparison with transpulmonary thermodilution. Br J Anaesth. 2015;115(1):53–60.
15. Pamminger M, Reindl M, Kranewitter C, et al. Prognostic value of pulmonary transit time by cardiac magnetic resonance imaging in ST-elevation myocardial infarction. Eur Radiol. 2023;33(2):1219–28.
16. Li P, Jin L, Feng L, et al. ICAM-1-carrying targeted nano contrast agent for evaluating inflammatory injury in rabbits with atherosclerosis. Sci Rep. 2021;11(1):16508.
17. Raskob GE, Angchaisuksiri P, Blanco AN, et al. Thrombosis: a major contributor to global disease burden. Arterioscler Thromb Vasc Biol. 2014;34(11):2363–71.
18. Konstantinides SV, Meyer G, Becattini C, et al. 2019 ESC Guidelines for the diagnosis and management of acute pulmonary embolism developed in collaboration with the European Respiratory Society (ERS): The Task Force for the diagnosis and management of acute pulmonary embolism of the European Society of Cardiology (ESC). Eur Respir J. 2019;54(3):1901647.
19. Wendelboe AM, Raskob GE. Global Burden of Thrombosis: Epidemiologic Aspects. Circ Res. 2016;118(9):1340–7.
20. de Miguel-Díez J, Jiménez-García R, Jiménez D, et al. Trends in hospital admissions for pulmonary embolism in Spain from 2002 to 2011. Eur Respir J. 2014;44(4):942–50.
21. Dentali F, Ageno W, Pomero F, et al. Time trends and case fatality rate of in-hospital treated pulmonary embolism during 11 years of observation in Northwestern Italy. Thromb Haemost. 2016;115(2):399–405.
22. Lehnert P, Lange T, Møller CH, et al. Acute Pulmonary Embolism in a National Danish Cohort: Increasing Incidence and Decreasing Mortality. Thromb Haemost. 2018;118(3):539–46.
23. Wiener RS, Schwartz LM, Woloshin S. Time trends in pulmonary embolism in the United States: evidence of overdiagnosis. Arch Intern Med. 2011;171(9):831–7.
24. Shiraev TP, Omari A, Rushworth RL. Trends in pulmonary embolism morbidity and mortality in Australia. Thromb Res. 2013;132(1):19–25.
25. Kempny A, McCabe C, Dimopoulos K, et al. Incidence, mortality and bleeding rates associated with pulmonary embolism in England between 1997 and 2015. Int J Cardiol. 2019;277:229–34.
26. Pallela VR, Thakur ML, Consigny PM, et al. Imaging thromboembolism with Tc-99m-labeled thrombospondin receptor analogs TP-1201 and TP-1300. Thromb Res. 1999;93(4):191–202.
27. Tang Z, Wang X, Huang J, et al. Gene Expression Profiling of Pulmonary Artery in a Rabbit Model of Pulmonary Thromboembolism. PLoS ONE. 2016;11(10): e0164530.
28. Streitberger A, Modler P, Häggström J. Increased normalized pulmonary transit times and pulmonary blood volumes in cardiomyopathic cats with or without congestive heart failure. J Vet Cardiol. 2015;17(1):25–33.
29. Morita T, Nakamura K, Osuga T, et al. Evaluation of Right Ventricular Function and Dyssynchrony in a Dog Model of Acute Pulmonary Embolism: Diagnostic Utility and Reversibility. Front Vet Sci. 2022;9: 861064.
30. Yildiz M, Karakoyun S, Acar RD, et al. Effectiveness of low-dose prolonged infusion of tissue plasminogen activator in a nonagenarian patient with acute pulmonary embolism and main pulmonary artery thrombus. Blood Coagul Fibrinolysis. 2013;24(1):95–6.
31. Lankhaar JW, Westerhof N, Faes TJ, et al. Quantification of right ventricular afterload in patients with and without pulmonary hypertension. Am J Physiol Heart Circ Physiol. 2006;291(4):H1731-1737.
32. Decai ZENG, Ji WU, Hui CHEN, et al. Correlation Between the Size of Thrombus and Right Ventricular Function Using Echocardiography in Rabbit with Acute Pulmonary Embolism. Chinese Journal of Medical Imaging. 2018;26(05):327–30+335.
33. Lakoma A, Tuite D, Sheehan J, et al. Measurement of pulmonary circulation parameters using time-resolved MR angiography in patients after Ross procedure. AJR Am J Roentgenol. 2010;194(4):912–9.
34. Colin GC, Pouleur AC, Gerber BL, et al. Pulmonary hypertension detection by computed tomography pulmonary transit time in heart failure with reduced ejection fraction. Eur Heart J Cardiovasc Imaging. 2020;21(11):1291–8.
35. Zhao H, Tsauo J, Zhang X, et al. Pulmonary transit time derived from pulmonary angiography for the diagnosis of hepatopulmonary syndrome. Liver Int. 2018;38(11):1974–81.
36. Jones RH, Sabiston DC Jr, Bates BB, et al. Quantitative radionuclide angiocardiography for determination of chamber to chamber cardiac transit times. Am J Cardiol. 1972;30(8):855–64.
37. Selzer A, Dunlap RW, Wray HW, et al. A critical appraisal of the circulation time test. Arch Intern Med. 1968;122(6):491–5.
38. Wu YW, Hsu PY, Lin YH, et al. Diagnostic and Prognostic Implications of Exercise Treadmill and Rest First-Pass Radionuclide Angiography in Patients With Pulmonary Hypertension. Clin Nucl Med. 2017;42(9):e392–9.
39. Saporito S, Herold IH, Houthuizen P, et al. Model-Based Characterization of the Transpulmonary Circulation by Dynamic Contrast-Enhanced

Magnetic Resonance Imaging in Heart Failure and Healthy Volunteers. Invest Radiol. 2016;51(11):720–7.
40. Monahan K, Coffin S, Lawson M, et al. Pulmonary transit time from contrast echocardiography and cardiac magnetic resonance imaging: Comparison between modalities and the impact of region of interest characteristics. Echocardiography. 2019;36(1):119–24.
41. Herold IH, Saporito S, Mischi M, et al. Pulmonary transit time measurement by contrast-enhanced ultrasound in left ventricular dyssynchrony. Echo Res Pract. 2016;3(2):35–43.
42. Kang S, Chen J, Zhang H, et al. Pulmonary Transit Time Assessment by CEUS in Healthy Rabbits: Feasibility, and the Effects of UCAs Dilution Concentration. Ultrason Imaging. 2024;46(3):178–85.
43. Piscaglia F, Bolondi L. The safety of Sonovue in abdominal applications: retrospective analysis of 23188 investigations. Ultrasound Med Biol. 2006;32(9):1369–75.
44. Bokor D. Diagnostic efficacy of SonoVue. Am J Cardiol. 2000;86(4a):19g–24g.
45. Sugiura E, Dohi K, Onishi K, et al. Reversible right ventricular regional non-uniformity quantified by speckle-tracking strain imaging in patients with acute pulmonary thromboembolism. J Am Soc Echocardiogr. 2009;22(12):1353–9.

## Publisher's Note